

Authors' Accepted Manuscript

this is the authors version of the article:

Effect of sliding speed and counterface properties on the tribo-oxidation of brush seal material under dry sliding conditions

M.R. Thakare^{*1}, J. F. Mason², A.K. Owen¹, D.R.H. Gillespie¹, A. J. Wilkinson², G. Franceschini³

1. Osney Thermofluids Laboratory (Southwell Building), Department of Engineering Science, University of Oxford, Parks Road, Oxford, OX1 3PJ, U.K

2. Department of Materials, University of Oxford, Parks Road, Oxford, OX1 3PH, U.K

3. Transmissions, Structures and Drives, Rolls-Royce plc, Moor Lane, Derby, DE24 8BJ, U.K

The version of record appears in

Tribology International

Volume 96, April 2016, Pages 373–381

<http://dx.doi.org/10.1016/j.triboint.2013.02.010>



Effect of sliding speed and counterface properties on the tribo-oxidation of brush seal material under dry sliding conditions

M.R. Thakare^{*1}, J. F. Mason², A.K. Owen¹, D.R.H. Gillespie¹, A. J. Wilkinson², G. Franceschini³

1. Osney Thermofluids Laboratory (Southwell Building), Department of Engineering Science, University of Oxford, Parks Road, Oxford, OX1 3PJ, U.K

2. Department of Materials, University of Oxford, Parks Road, Oxford, OX1 3PH, U.K

3. Transmissions, Structures and Drives, Rolls-Royce plc, Moor Lane, Derby, DE24 8BJ, U.K

Abstract

The performance of dynamic seals and hence the overall efficiency of the gas turbine is strongly dependent on the wear of individual seal elements and their ability to provide continuous sealing. Dynamic seals such as brush seals contact the rotating 'rotor' during operation, either transiently or continuously depending on factors such as thermal expansions, axial/radial displacements and eccentricities of the rotating components. This intermittent or continuous contact results in sliding wear of the seal tips and dictates the seal degradation and hence its efficiency.

The present work examines the effect of sliding speeds between 6 m s⁻¹ and 150 m s⁻¹ on the wear-oxidation of Haynes 25 brush seal 'tufts' sliding against nitrided steel and thermal sprayed chrome oxide coating.

* Dr. Mandar R. Thakare, Osney Thermofluids Laboratory, Department of Engineering Science, University of Oxford, Parks Road, Oxford, OX1 3PJ, UK. Tel: +44 (0)1865288760, Email: mandar.thakare@eng.ox.ac.uk

Introduction

Gas turbine engines work on the principle of momentum imbalance created as a result of the high exhaust velocity compared to the low intake velocity. The intake air entering the core of the gas turbine engine is divided as the primary air flow, which passes through the combustor and gas stream, and the secondary air flow, which is used for applications such as internal cooling, external bleed for cabin air conditioning and accessory devices. A reduction in secondary air flow leakage past seals can result in approximately 4–6% increase in power together with reducing specific fuel consumption by 3–5% [1] and [2]. Dynamic seals such as labyrinth seals and brush seals are used to reduce air flow leakages in secondary air systems. The main advantage of using brush seals in place of labyrinth seals is their ability to accommodate transient shaft excursions due to an increased compliance which can lead to a significant reduction in leakage rates [3]. A schematic of a brush seal cross-section and side view identifying all the key features is shown in Fig. 1.

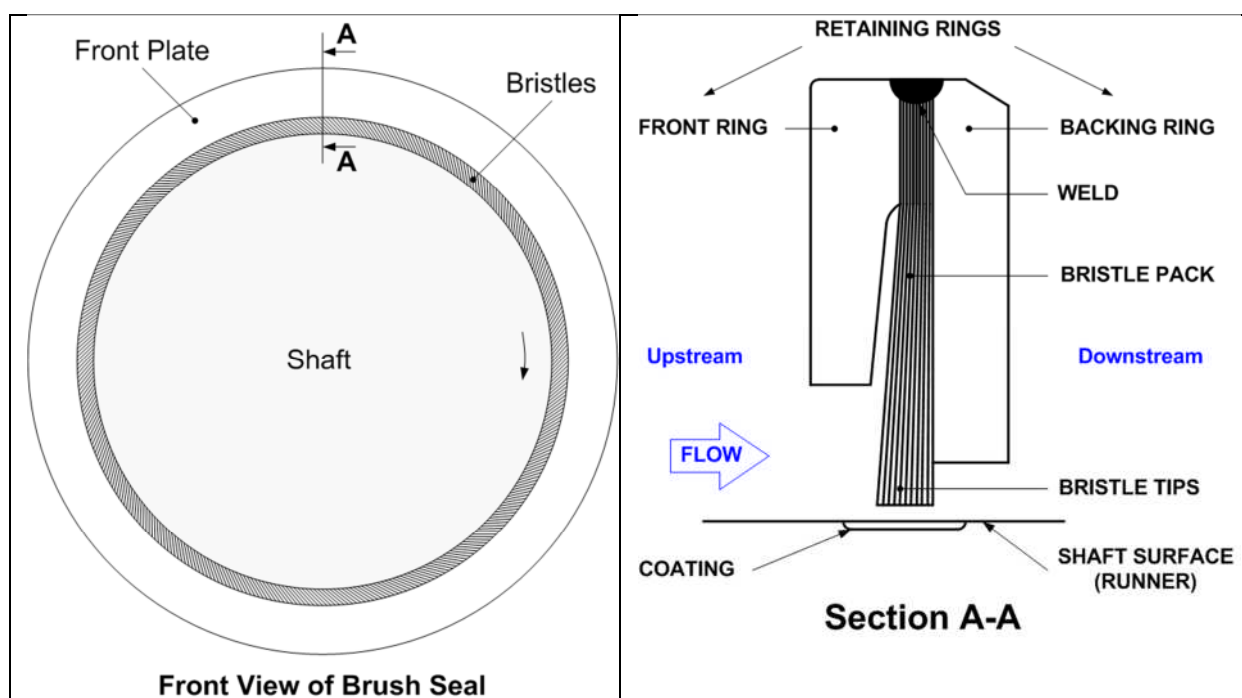


Figure 1: (a) Schematic of the front view of brush seal showing the relative position of bristles and the shaft (b) Cross sectional view across A-A section showing the position of bristles and shaft relative to the gas flow.

Individual bristles are oriented to the shaft with a lay angle (typically around 45°) pointing in the direction of rotation. Despite the increased compliance, bristles may contact the rotor transiently or continuously during operation and this contact can result in wear of individual bristles resulting in an increase in leakage between the seal and the rotor. Brush seals are expected to perform under a wide range of operating conditions with speeds up to 450 m s⁻¹ [1] and tip loads up to 70 kPa [2] in ambient temperatures up to 800 °C [1] and [2]. These extreme speeds and temperatures, which are often difficult to replicate in controlled laboratory conditions, make tribological evaluation of candidate brush seal materials very challenging. Most of the work reported on tribological evaluation of brush seals [2] and [4] has been done at high temperatures, albeit at much lower sliding speeds. The general assumption under such conditions being that ambient temperature has a greater effect on dry sliding wear between the bristles and the rotor than sliding speed. In the present work, tribological tests are conducted at ambient temperatures but at representative sliding

speeds. At high sliding speeds, the frictional heat generated is likely to dominate the thermal field at the sliding interface.

Background

The nature of this localised heating and the generation of the resultant “flash” temperature has been extensively investigated by Bowden and Tabor [5], Archard [6], Blok [7] and Ashby et al. [8]. This local heating is likely to influence the oxidation and hence the wear-mechanisms experienced during dry-sliding wear. The effect of speed on dry sliding wear from a mechanistic perspective was initiated by Archard and Hirst [9]. They identified mild and severe wear as two distinct mechanisms during unlubricated sliding of metallic surfaces. The distinction between the two wear modes was down to the size and mechanism of the formation of delaminated debris. Hirst and Lancaster [10], [11], [12], [13] and [14] examined the effects of parameters such load, speed and surface roughness on the change in wear rates and concluded that the transition from severe wear to mild wear occurred when the rate of formation of surface films was greater than the rate of material removal by intermetallic contact and delamination of debris.

The role of oxidation in high speed dry sliding was also investigated by Cocks [15] and [16], who observed that there is another mechanism that is likely to occur whereby an increase in load or speed resulted in disintegration within the oxide film and this potentially leads to a sharp rise in wear rates. This behaviour was influenced by factors such as geometry of the tribo-pair and the relative hardness ratio between the metal and its oxide. Rigney et al. [17] and [18] developed a model to predict the delamination of flaky debris in the wear interface based on the shear strength between the oxide layers and substrates. They also identified the possibility of material transfer between the tribo-pairs and the formation of a transfer film on one or both surfaces during dry sliding. They further proposed that these were formed as a result of a three-step process involving (a) formation of elongated and ultrafine grained microstructure near the surface due to high levels of plastic strains, (b) delamination and mixing with the counterface material and (c) stabilising by mechanical alloying with a second phase, all of which depended on factors such as load, sliding speed and relative hardness ratio between the tribo-pairs. Direct observations of the glazed layer were made by Inman et al. [19]. They studied a nickel based superalloy after sliding against Stellite at elevated temperatures using Transmission electron microscopy (TEM). The glazed layers were characterized by a grain size of around 10 nm and composed of mixed oxides and metal particles. A mechanical mixing mechanism similar to that above was proposed. The benefits of a nano-structured layer were recognised by Kato and co-workers. They introduced a range of metal oxide nano-particles to the wear track [20] and found that a mild wear regime was established for those oxides with the higher diffusion coefficients and observed coherent tribo-films being formed. They also looked at self-generating tribo-films in various wear couples [21] and produced films ~40 µm thick in steel on steel which had a higher hardness than the parent metal.

Stott and Wood [22] examined the influence of oxidation on the formation of surface films and defined a stable compacted film as a “glazed” layer. They proposed that formation, agglomeration and compaction of oxide debris glazed layers results in ‘sintering’ of the material to form hard and compacted layers on the wearing surfaces, often leading to a decrease in wear and friction with an increase in test temperature and time. Jiang et al. [23] and [24] further expanded on this by identifying the ability of oxide debris to be re-entrained in the contact as the key parameter

responsible for the formation of a glazed layer. They further developed a mathematical model for capturing the transition from severe to mild wear based on the probability of wear debris particles entraining in the interface. As the probability of debris entrainment and compacting was higher for low speed and high temperature conditions, the formation of a glazed layer was mostly observed under such conditions.

There is a limited literature devoted to high sliding speeds although all involve much higher contact pressures than those used in this work. Montgomery [25] made an extensive study of various wear couples for gun barrel and projectile applications using a pin on disc arrangement at sliding speeds up to 457 m/s and contact pressures in the range 6.2–162 MPa. The energy input was seen as the key parameter and for low Normal pressure x velocity values friction tended to be erratic and wear rates high whereas at higher PV values friction and wear was more stable and wear rates lower. Philippon et al. [26] studied friction in the range 1–60 m/s and found that low friction correlated with the higher pressure and sliding speed combinations. Qiu et al. investigated the effect of atmosphere on wear and friction [27] and found both were improved by the presence of O₂. In a later study they made an estimate of the contact temperature For Titanium against steel and speeds in the range 30–70 m/s [28]. Temperature estimates were ~1000 °C for the higher speeds and pressures. Wear rates were also high this was attributed to unstable oxide films. Song et al. [29] tested a tungsten carbide/steel composite against steel at speeds up to 80 m/s. Wear rates increased rapidly above 60 m/s this was attributed to increased oxidation rates.

In their review of dry sliding wear mechanisms under a wide range of load-speed conditions for steel on steel, Lim and Ashby [30] identified two distinct regimes for oxidation-dominated wear as mild and severe, where these refer to levels of oxidation. In the load-speed space, mild oxidative wear was likely to occur when there is sufficient frictional heat to generate an oxide film to reduce asperity contact. A transition to severe oxidative wear was expected to occur when the asperities have completely oxidised creating a thin layer of molten oxide separating them.

It is clear that the wear mechanisms and the nature of the tribo-films formed depend significantly on the oxidation characteristics of the sliding surfaces as well as the mechanical alloying between various species present on the surfaces. It is therefore necessary to examine the exact nature of wear mechanisms likely to occur when dynamic seals are worn against wear resistant surfaces. Furthermore, the intricate geometry of brush seals is likely to alter the nature of debris entrainment as compared to standard pins used in most of the papers reported in the literature adding an extra complexity to the wear mechanisms.

Experimental

To examine the effects of sliding speed on tribo-oxidation of bristles and to mimic the contact conditions experienced during operation, a bristle ‘tuft’ comprising of a fixed number of individual bristles was prepared and used instead of a conventional pin in a pin-on-disc type tester. Bristles in the tuft were tilted at an angle consistent with the lay angle of brush seal elements used in an actual dynamic seal. A rubber sleeve was used to pack the bristles together and this tuft was clamped in a holder using grub screws. Closely packing multiple bristles in a tuft improved its rigidity and allowed contact pressure applied at bristle

tips to be accurately measured by mounting the tuft in a load cell. Fig. 2 shows a schematic of the brush seal tuft used in this test programme.

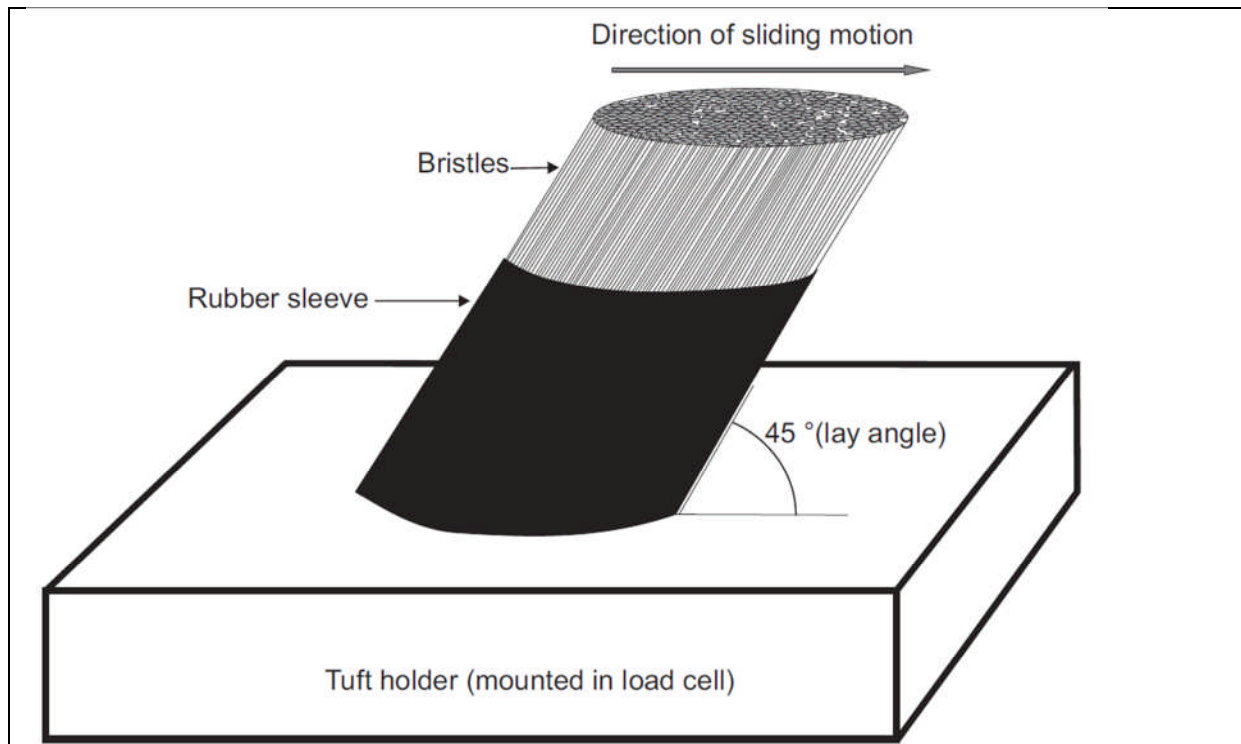


Figure 2: Bristle ‘tuft’ schematic showing the closed packed bristles and direction of sliding relative to the lay angle.

The sliding wear test rig comprised of a rotating disc powered by an air motor and the brush seal tuft mounted in a load cell loaded against this rotating disc using a DC motor as shown in Fig. 3. The load cell holding the tuft provided the measure of the exact load being applied at the wear-interface. A torque sensor connected between the air motor and the rotating disc provided a measure of the change in torque and could be used along with the measured load to compute friction. A digital dial gauge contacting the load cell was used to monitor the position of the tuft relative to the disc. Wear rates were computed from the change in tuft assembly position with time. Alterations in dial gauge reading as a result of thermal expansions in the apparatus and tuft due to frictional heating were excluded by ignoring data for the first 90 min of the test. It is expected that a thermal equilibrium (steady-state) is achieved after the first hour of testing. The total test duration was approximately five hours. Where required, 2D and 3D profilometry was used to measure the wear on the discs to compute the disc component of the total wear measured using the digital dial gauge during a test. An uncertainty analysis was undertaken in order to give an indication of the confidence of the measured data. 95% confidence intervals were estimated for the measured and calculated results following the procedures outlined in the ASME PTC19.1 standard [31].

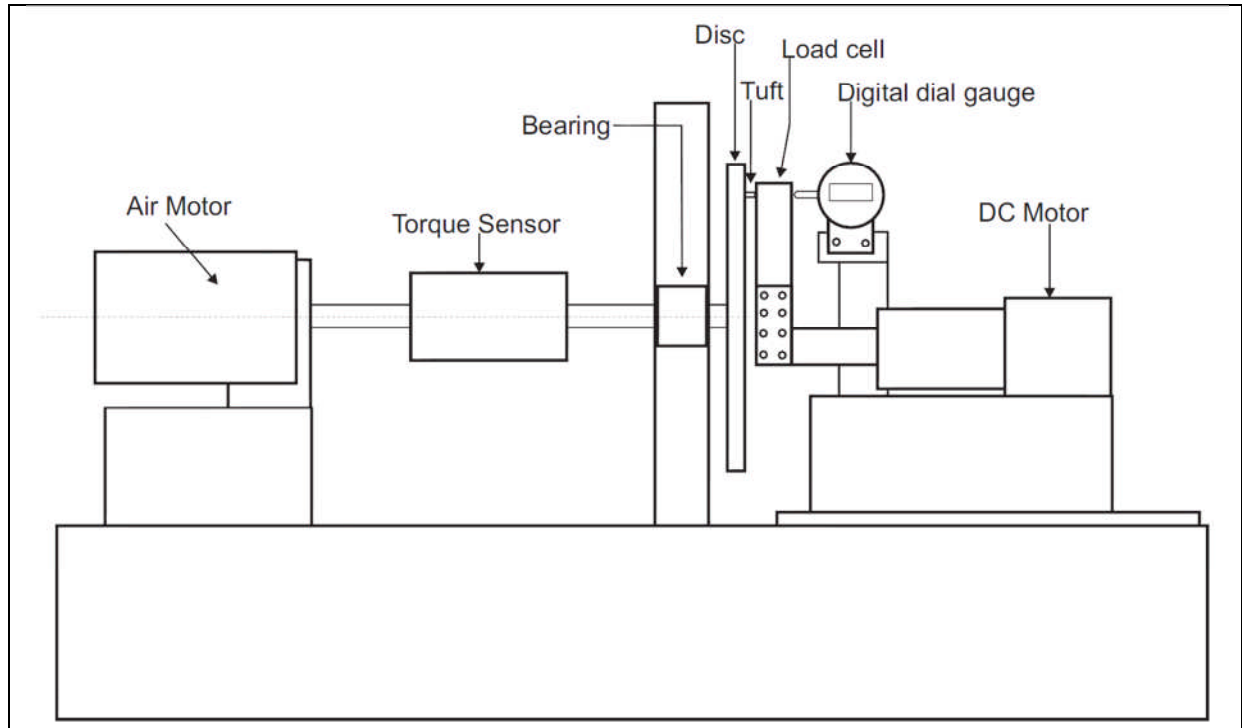


Figure 3: High speed tribology rig schematic.

For this study, brush seal tufts were worn against a nitride steel disc and chrome oxide coated disc at 6 m s⁻¹, 60 m s⁻¹ and 150 m s⁻¹. All tufts used in the test programme were made from commercial Haynes 25 alloy bristles of 0.1 mm diameter. Nominal composition of Haynes 25 alloy is given in Table 1.

Table 1: Nominal composition of Haynes 25 alloy as provided by the manufacturer

Element	C	Fe	Ni	Cr	Co	W	Mn	Si
% Weight	0.1	3*	10	20	51**	15	1.5	0.4*

* Maximum, ** As balance

Prior to testing, the bristle tufts were ground and cleaned ultrasonically. To allow for a clear distinction between a ground and a worn surface, tufts were ground in a direction perpendicular to the direction of motion during wear testing. Worn tufts were examined using a ZEISS Environmental Scanning Electron Microscope (ESEM) for identification of primary wear mechanisms and conducting Energy Dispersive X-ray (EDX) analysis for qualitative analysis of local chemistry. An Alicona 3D non-contact profilometer was also used to measure local surface features on worn surfaces. For a more detailed analysis of compositional variation with depth, representative bristles showing typical surface features were subjected to SIMS analysis using Ga ion bombardment across a 30 µm area at 1 nm s⁻¹ depth rate.

Additionally, the fine structure of the worn bristle surface and subsurface was examined using Transmission Electron Microscopy (TEM). Individual bristles showing typical surface morphologies were selected for TEM examination. Electron transparent foils were prepared using Focussed Ion Beam (FIB) instruments. The foils were normal to the worn surface and parallel to the direction of sliding. Several foils were prepared in a single bristle and were located approximately centrally in relation to the bristle and on a common axis parallel to the sliding direction. Initially a strip of

platinum was laid down by sputter coating in the same instrument. This was intended to protect the surface from erosion during the subsequent machining operations. The bristle material was then removed by progressively more precise FIB machining operations to produce a foil in-situ.

The foils were examined in a Phillips CM20 transmission microscope using bright field diffraction contrast to image the microstructure. The chemical composition of the features was determined using an Oxford Instruments EDX analysis using a beam focussed on the sample. The resolution of this technique was ~ 30 nm.

Results

Fig. 4 shows Specific Wear Rates (SWR, $\text{m}^3 \text{N}^{-1} \text{m}^{-1}$) calculated for Haynes 25 tufts worn against nitrided steel and chrome oxide coating at the three test speeds. The results appear to show two clear trends.

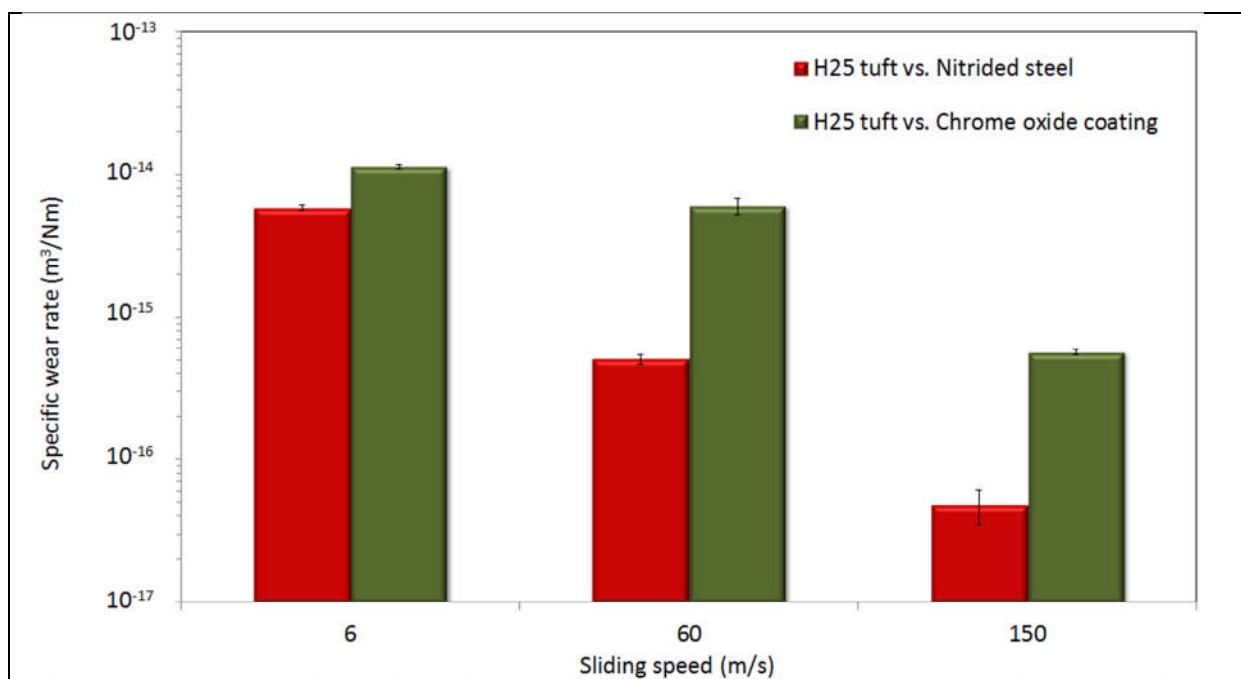


Figure 4: Specific wear rates observed for Haynes 25 bristle tufts worn against nitrided steel and chrome oxide coating at 6 m s^{-1} , 60 m s^{-1} and 150 m s^{-1} .

First, an increase in speed appears to have resulted in a decrease in wear rates. To confirm that this effect is not due to an increase in sliding distance, some of the data were replotted to show wear volume versus sliding distance, see Fig. 5. Clearly, the three lines show different slopes confirming that the decrease in SWR is not due to an increase in the sliding distance, but has to do with the underlying wear mechanisms which are examined subsequently. Secondly, Haynes 25 tufts worn against chrome oxide coating consistently show higher wear compared to the tufts worn against nitrided steel.

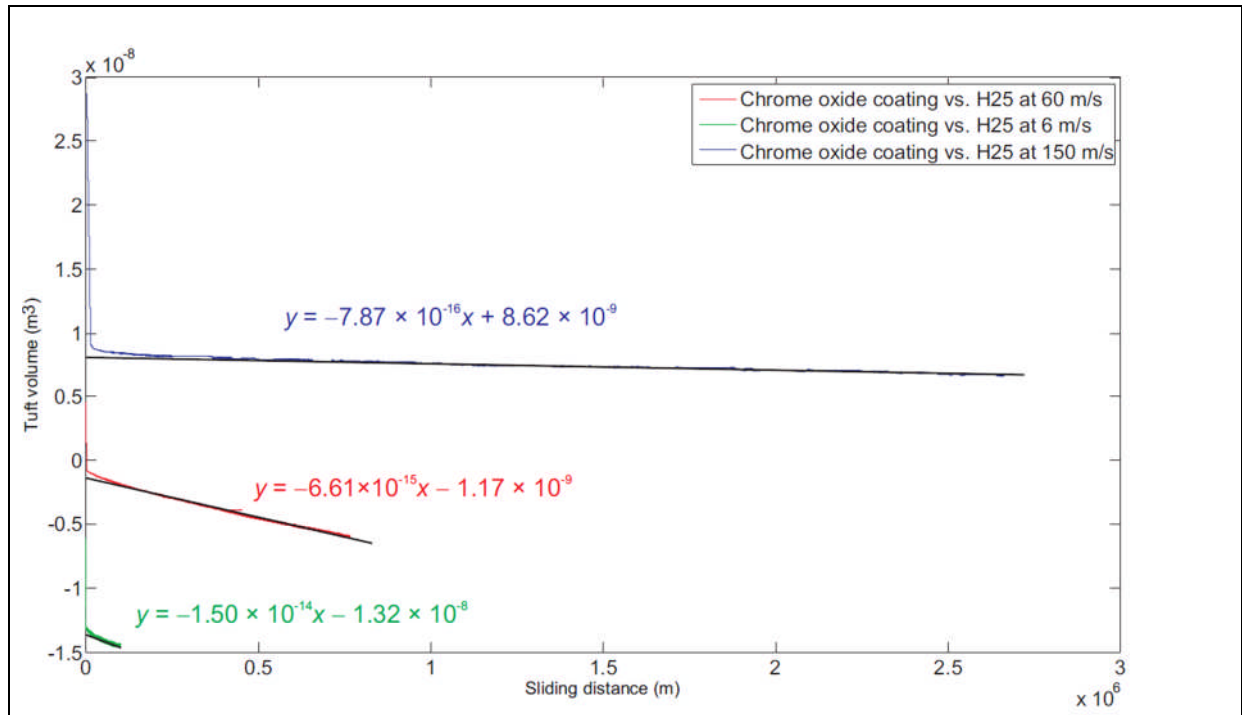


Figure 5: Data for Haynes 25 tuft vs. chrome oxide coating replotted to show variation in slope for the three lines corresponding to the three speeds tested.

To understand these trends, all tufts were examined under a SEM. Representative micrographs from the tufts are shown in Fig. 6 with prominent features having been highlighted. For comparison, all micrographs are at the same magnification and have been oriented such that the direction of relative motion of the rotor surface was from right to left. All surfaces show evidence of plastic deformation and the formation of what looks like a "comet tail" consistent with the direction of motion. This is a common feature that has been observed in all micrographs and indicates local plastic flow within the tuft surface. Some bristles also show evidence of scratching along the surface consistent with the direction of motion. These scratches appear to be similar to two-body grooving observed during abrasive wear. In addition to the plastic flow and scratching, the tufts worn against nitrided steel show evidence of partially formed tribo-films (Fig. 6b) and delaminated regions. Tufts worn against nitrided steel also show evidence of debris being trapped between bristle interstices, possibly due to the entrainment of delaminated tribo-films. The scratches observed on the tufts worn against nitrided steels are also likely to be as a result of entrainment of delaminated tribo-film fragments. An increase in speed also appears to have altered the nature of the trapped debris for the tufts worn against nitrided steel, see Fig. 6a–c. While the tuft worn at 6 m s⁻¹ show loose debris trapped in the bristle interstices, the debris in the tuft worn at 150 m s⁻¹ appear to have compacted and sintered. The tufts worn against the chrome oxide coating at 6 m s⁻¹ and 150 m s⁻¹ show features similar to those observed on tufts worn against nitrided steel. However, the tuft worn against chrome oxide coating at 60 m s⁻¹ shows a very different morphology with no evidence of a partially delaminated tribo-film.

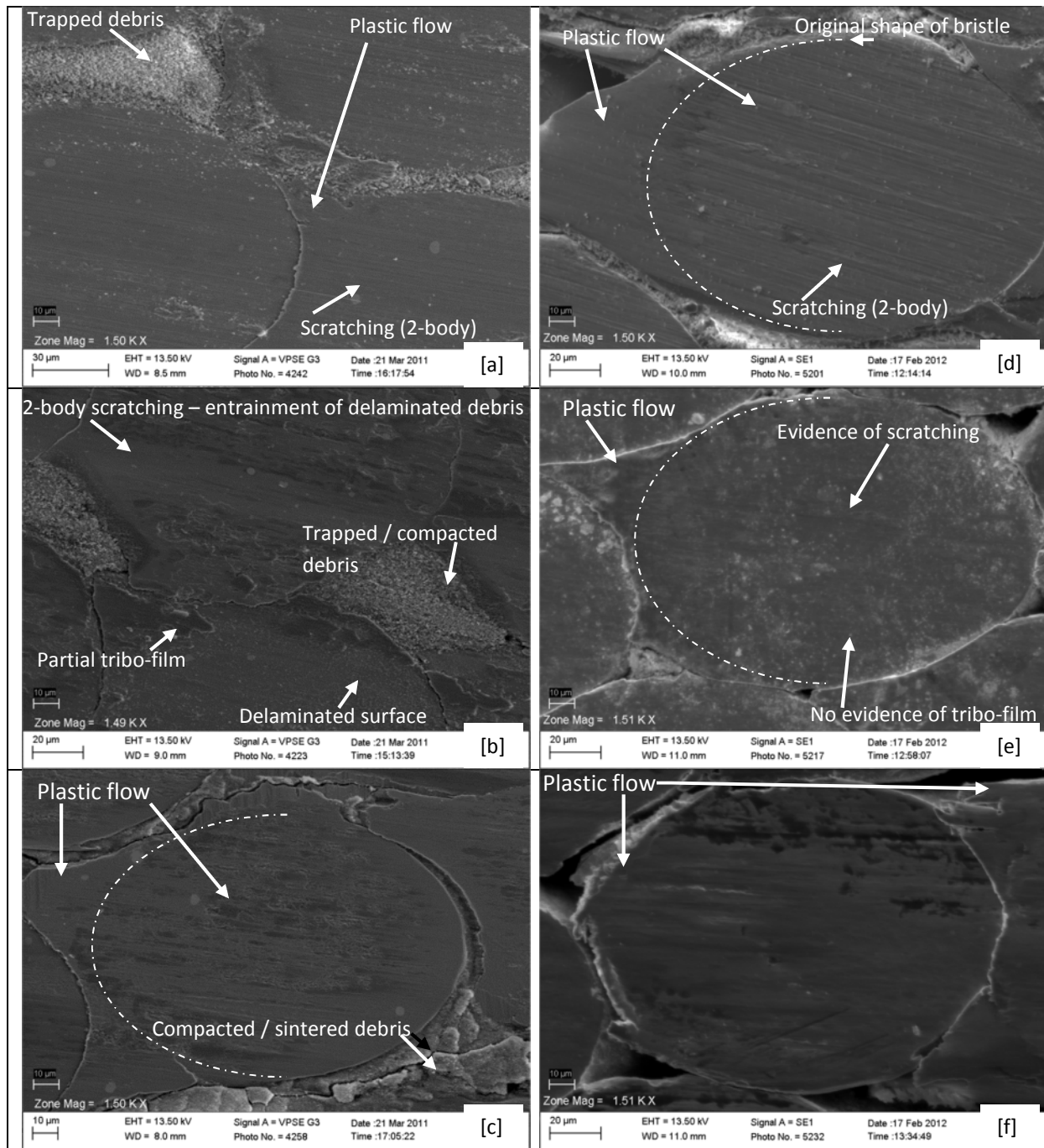


Figure 6: Effect of sliding speed on wear mechanism observed on Haynes 25 bristle tufts worn at (a) 6 m s^{-1} vs. nitrided steel, (b) 60 m s^{-1} vs. nitrided steel, (c) 150 m s^{-1} vs. nitrided steel, (d) 6 m s^{-1} vs. chrome oxide coating, (e) 60 m s^{-1} vs. chrome oxide coating and (f) 150 m s^{-1} vs. chrome oxide coating. For all micrographs, relative direction of motion was from right to left.

Energy Dispersive X-ray (EDX) analysis was also conducted on all bristle tufts using identical conditions. Fig. 7a shows the proportion of elements (by weight %) for the three tufts worn against nitrided steel at 6 m s^{-1} , 60 m s^{-1} and 150 m s^{-1} . For comparison, EDX analysis from an unworn Haynes 25 tuft is also included in the graph and is found to be consistent

with its base composition. Interestingly, the proportion of oxygen and iron appear to increase with speed along with a corresponding decrease in the proportion of all other elements. The additional iron is expected to be from the nitrided steel counterface. In contrast, the tufts worn against the chrome oxide do not show any increase in the iron content, see Fig. 7b. They do show increased oxygen content for the worn tufts, however there is no obvious speed dependency in the proportion of oxygen detected, as was the case with tufts worn against nitrided steel.

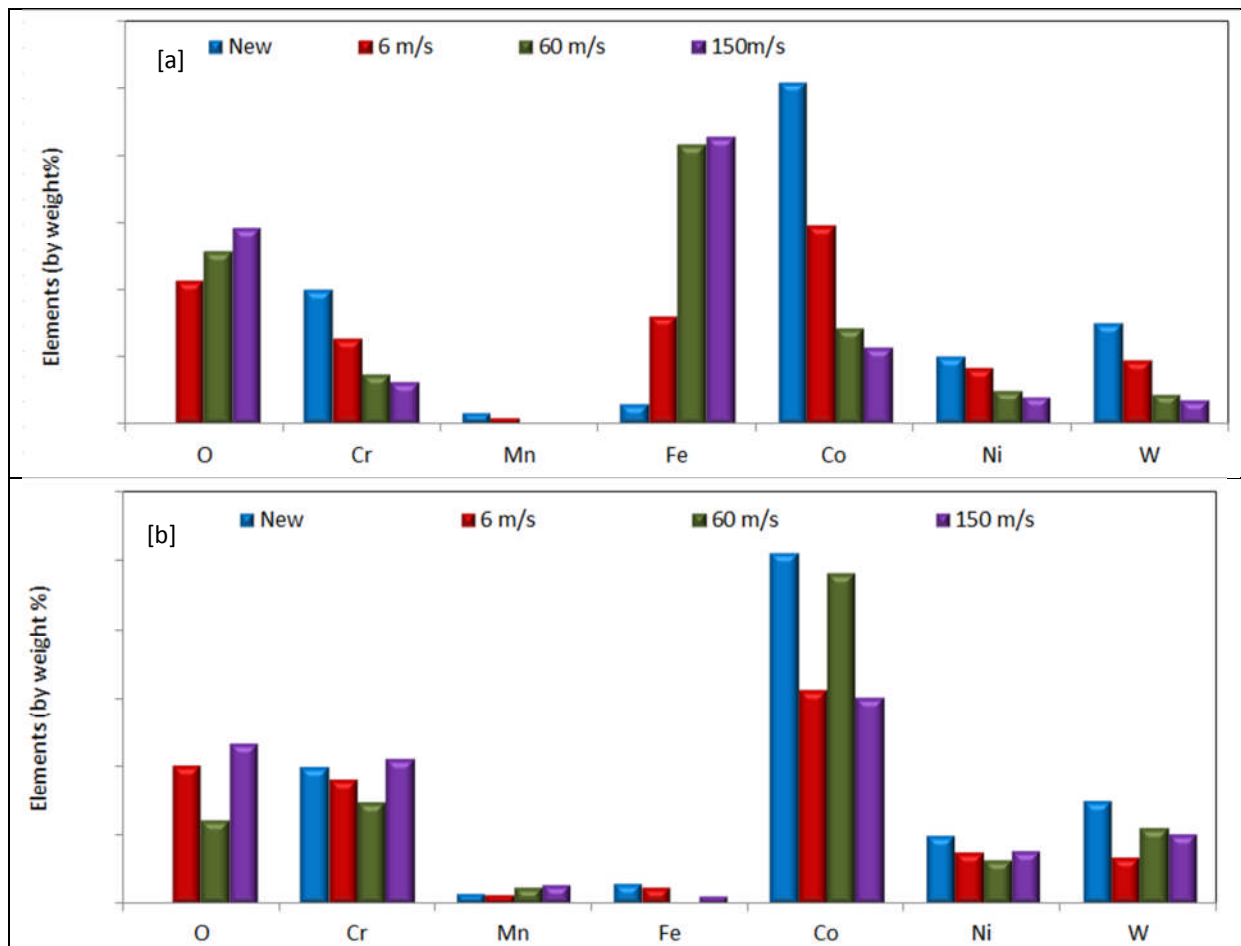


Figure 7: (a) Haynes 25 tuft worn against nitrided steel and (b) Haynes 25 tufts worn against chrome oxide coating.

A more detailed analysis of depthwise surface chemistry was achieved by using SIMS on individual bristles extracted from each tuft (each bristle selected showed a representative surface appearance). Fig. 8 compares the negative ions detected during SIMS analysis on all bristles bombarded with Ga ions over a 30 μm area at a sputtering rate of 1 nm s⁻¹. For consistency, the axes on all graphs are drawn to the same scale. Oxygen concentrations appear to reduce to a baseline value after a certain thickness, which may be indicative of the thickness of the possible tribo-films formed on the sample surfaces. For bristles worn at 6 m s⁻¹, baseline values appear to have reached around 200 nm depth from the surfaces. While the bristle worn against chrome oxide coating at 60 m s⁻¹ appears to show similar film thickness (200 nm), the bristle worn against nitrided steel seems to show a gentler

gradient of oxygen concentration, indicative of a thicker tribo-film. Interestingly, the data for the bristle worn against nitrided steel at 150 m s^{-1} show a steeper gradient with baseline values occurring in less than 100 nm from the surface. This could be suggestive of a thinner tribo-film. The bristle worn against chrome oxide coating on the other hand shows very little change in oxygen concentration with depth, possibly due to the absence of a coherent tribo-film

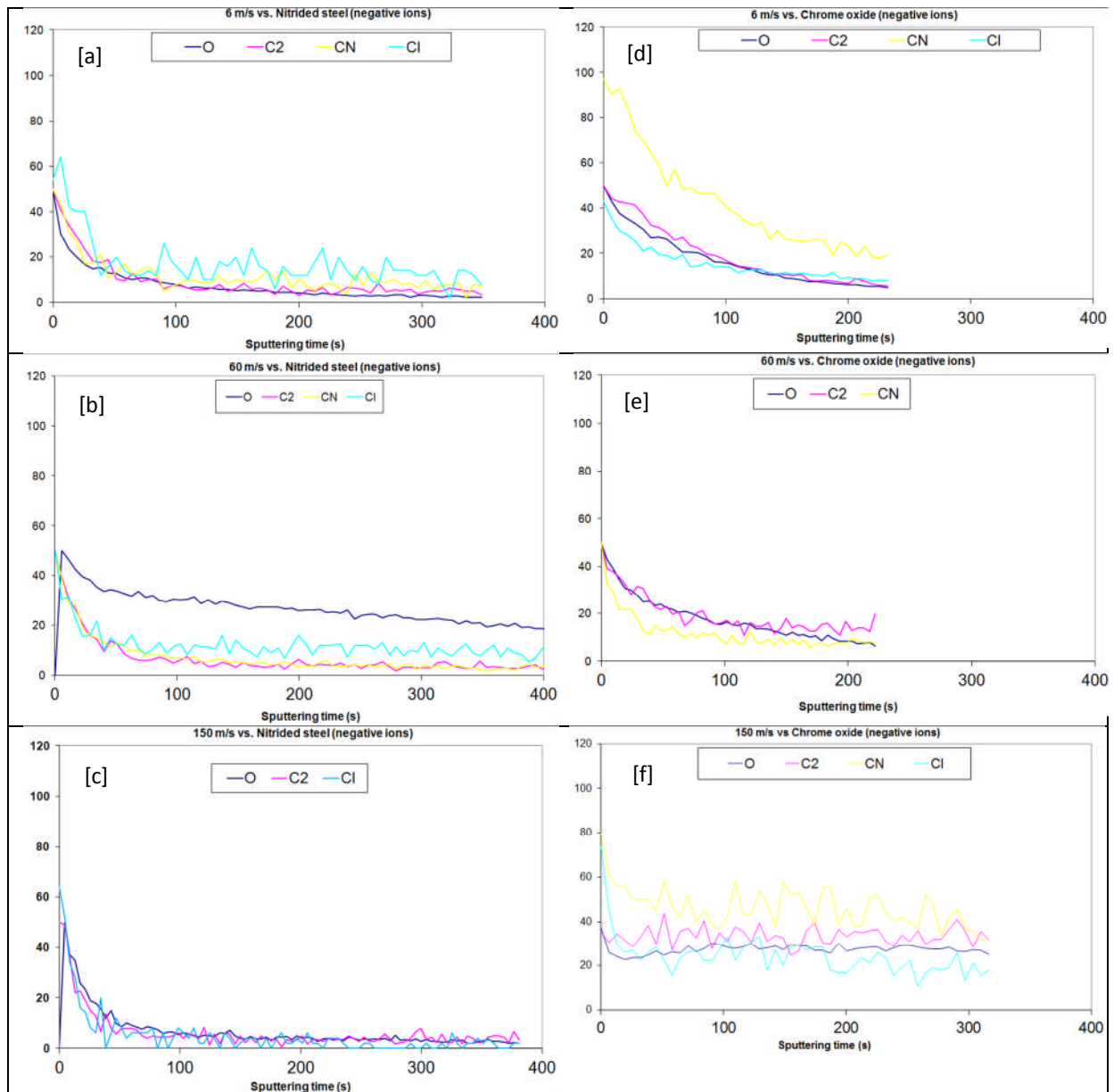


Figure 8 Negative ions detected during SIMS analysis on Haynes 25 bristles worn at (a) 6 m s^{-1} vs. nitrided steel, (b) 60 m s^{-1} vs. nitrided steel, (c) 150 m s^{-1} vs. nitrided steel, (d) 6 m s^{-1} vs. chrome oxide coating, (e) 60 m s^{-1} vs. chrome oxide coating and (f) 150 m s^{-1} vs. chrome oxide coating.

Fig. 9a and b shows TEM micrographs of two samples run at 60 m/s against nitrided steel and chrome oxide coated steel respectively. Both samples show similar characteristics, the wear interface is on the left, moving across the micrograph from left to right, four distinct layers are observed. With reference to the micrograph shown in Fig. 9a the following distinct layers are observed:

1. First there is a layer of amorphous platinum, laid down for protection as discussed in the Section 3. This may appear discontinuous as in some places it has been milled away all together.
2. Next, there is a fine grained layer about 100 nm thick which has a well-defined boundary with the substrate. The substructure of this layer is very fine, being composed of particles typically in the range 10–30 nm diameter. This is interpreted as being a “tribo-film” composed of particles removed, potentially from both sliding surfaces, and re-consolidated on the bristle surface. Further support for this view is provided by the chemical analysis shown in Fig. 11. The analysis of the tribo-film for the bristle worn against the nitrided steel shows large increases of iron and oxygen content in comparison the analysis of the substrate alloy, whereas the bristle worn against the chrome oxide coating shows a more modest increase in oxygen content and no significant increase iron content.
3. Below the fairly flat interface with the tribo-film, a recrystallised layer is observed. The average grain size is significantly larger than that of the tribo-film but is still fine at around 50–100 nm.
4. Lastly there is the unrecrystallised substrate which forms an irregular boundary with the recrystallised layer. In this sample the substrate structure is heavily deformed and the curvature introduced into the large crystal towards the top left is particularly striking.

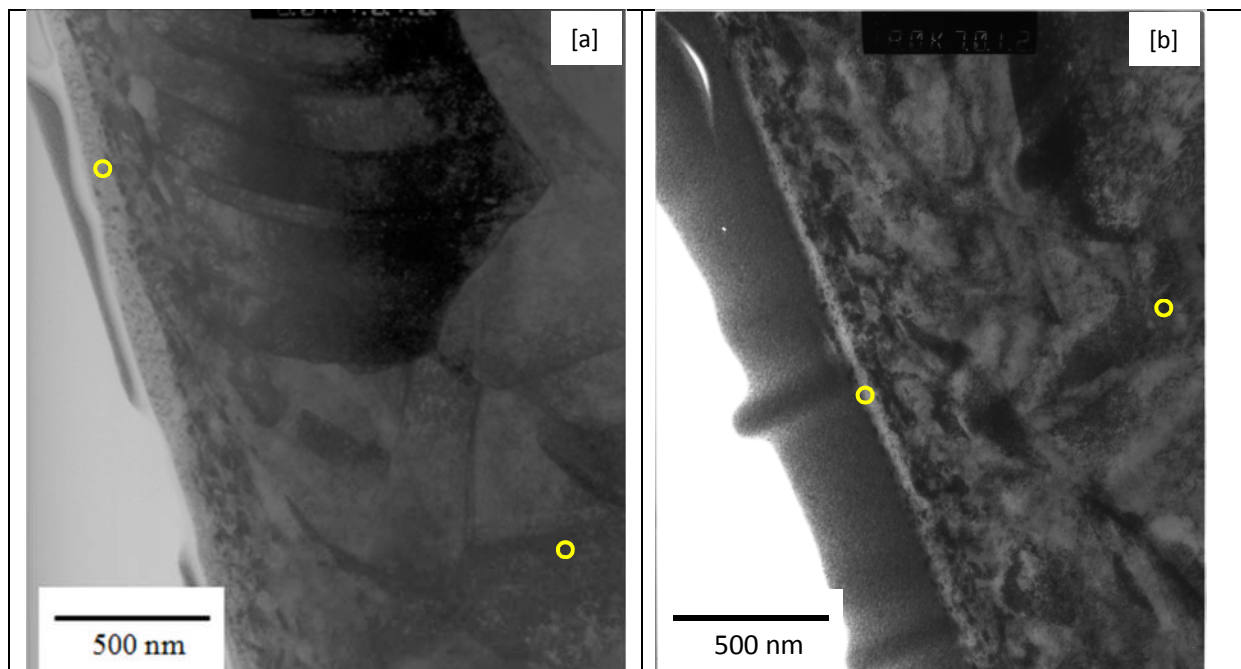


Figure 9: TEM micrographs for Haynes 25 tuft worn at 60 m s^{-1} against (a) nitrided steel disc and (b) chrome oxide coating.

The micrograph on the right (Fig. 9b) shows the microstructure of the bristle surface run against a hard chrome oxide coating. The micrograph is in the same orientation as the previous one and moving from left to right the following features are present:

1. Below the amorphous platinum strip there is a lighter band about 30–50 nm wide containing particles of a few tens of nanometres in diameter. Despite a fairly clearly defined boundary this region is not easy to distinguish microstructurally from the adjacent recrystallised part. However EDX analysis gives an increase in oxygen content for this band over the substrate composition, see Fig. 11. The balance of evidence therefore suggests that this is a deposited tribo-film.
2. The recrystallised region is similar in extent and microstructure to that of the sample run against nitrided steel.
3. The unrecrystallized substrate consists of equi-axed grains of a diameter up to a few microns. The average grain size measured for a sample of “as manufactured” wire was 1.7 μm .

Discussion

The following key observations can be made from the analysis of worn bristle tufts. The observations in relation to tribo-films are supported by corroborative data from several sources, in particular SEM, SEM-EDX, SIMS, TEM and profilometry.

1. An increase in sliding speed leads to a decrease in wear rates for both counterface materials and in general tufts worn against nitrided steel show lower wear compared to those worn against chrome oxide coating.
2. An increase in speed also seems to indicate increased levels of oxygen content and a more uniform distribution of surface films.
3. SIMS and TEM analysis shows that oxygen-rich tribo-films are generally tens to hundreds of nanometres thick.
4. In addition to tribo-films, worn surfaces also show significant levels of local plastic flow at the surface leading to the formation of "comet tail" type features. Sub-surface recrystallisation observed in the TEM is also indicative of high levels of local strains and temperatures close to melting point.
5. Furthermore, tribo-films formed on bristles worn against the nitrided steel show a significant increase in Fe content, indicative of material pick-up during sliding. This is not the case with the bristles worn against the chrome oxide coating.
6. Worn tufts show significant entrapment of debris in the bristle interstices. In terms of wear mechanisms, the presence of abrasive wear features on the surfaces also suggest that delamination and entrainment of tribo-film fragments is expected to result in abrasive wear. In general, wear mechanisms observed on the worn tufts can be summarised as oxidative wear of varying degrees and abrasive wear.

All the features observed on worn bristles have been summarised in a schematic of a bristle shown in Fig. 11. The schematic (not drawn to scale) identifies the local plastic flow seen on the surface and the recrystallised zone along with a discontinuous tribo-film. It was generally observed that an increase in the sliding speed resulted in the formation of an evenly distributed and well adhering tribo-film. Very little evidence of a stable tribo-film is seen at the lowest speed (6 m s^{-1}) and despite the oxygen content detected in SEM-EDX and SIMS, the surface tends to reveal predominantly two-body abrasive wear-like features, see Fig. 6a and d. An increase in speed to 60 m s^{-1} appears to result in the formation of a more visible, but discontinuous tribo-film. The discontinuities appear to have been formed as a result of local delamination also resulting in the formation of a fracture-like morphology on the delaminated surface as well as two-body grooving features, see Fig. 6b and e. With a further increase in speed, the level of distribution of the tribo-film on the surface appears to increase, see Fig. 6c and f.

Interestingly, the presence of unaffected parent grain microstructure below the recrystallisation zone and deformed grains also suggests that the effects of high speed sliding are confined to a layer a few microns thick below the wear interface. Oxidation tests on Haynes 25 wire samples done in a separate study not covered in this paper indicated that grain growth had not occurred in a sample heated in air to 1000°C and held for 24 h. The dynamic situation that would occur at the sliding interface where the material is simultaneously heated and deformed might be expected to assist recrystallisation and suppress the activation temperature a little but it is still a high temperature process. This indicates the presence of a steep thermal gradient along the bristle tuft.

Another interesting aspect is the effect of counterface composition on the nature and stability of the tribo-films. The comparison of SEM EDX data (Fig. 7) clearly shows an increased proportion of Fe in the bristles worn against nitrided steel, which is most likely to be a result of material transfer from the disc surface. Also, the proportion of Fe is significantly higher for tufts worn at 60 m s^{-1} and 150 m s^{-1} sliding speeds. The presence of a Fe-rich tribo-film on the bristles worn against nitrided steel is also confirmed by the EDX analysis done during TEM, see Fig. 10.

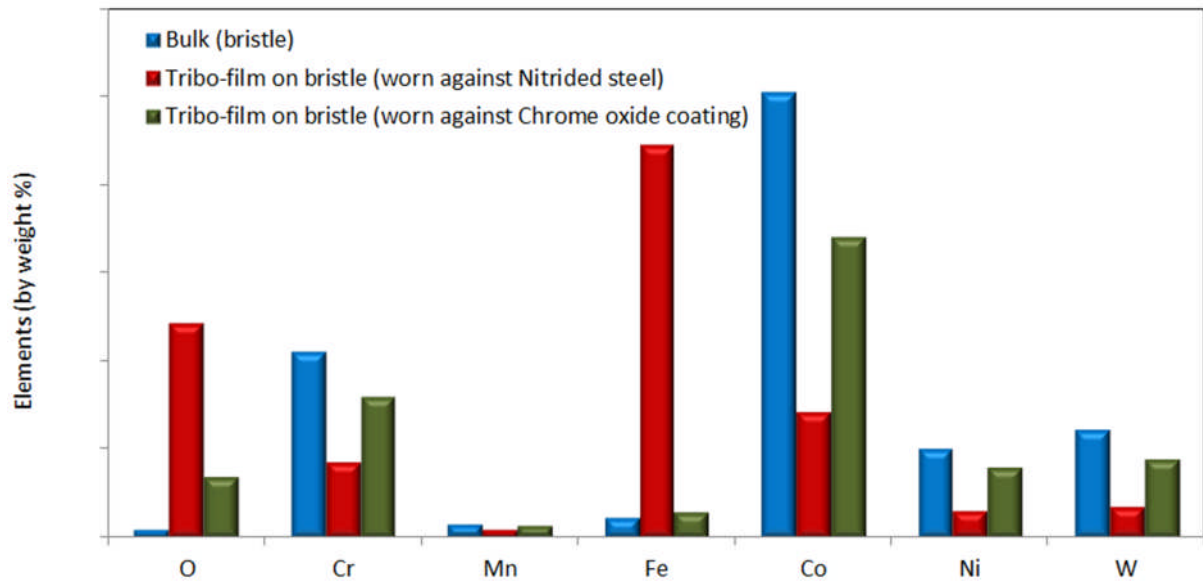


Figure 10: EDX analysis done on TEM foils at locations shown in Figure 10.

Not surprisingly, this increase in Fe content is not observed for bristles worn against the chrome oxide coating. The presence of oxygen on tufts worn against chrome oxide coating identified using SEM-EDX, SIMS and TEM-EDX also indicates that a Co and Cr rich tribo-film is likely to be present on the surface. As seen from the comparison of TEM cross-sections (Fig. 9), the tribo-film formed on the bristle worn against the chrome oxide coating is much thinner than the tribo-film formed on the bristle worn against the nitrided steel counterface. Surface profilometry measurements on the chrome oxide disc also indicated negligible wear on the discs, which may have also hindered the formation of a stable tribo-film. This can also be related to the reduced levels of debris trapped in bristle interstices for the tufts worn against the chrome oxide coating. Consequently, it could be said that the bristle vs. nitrided steel couple appears to show a greater propensity to form tribo-films as compared to the bristle vs. chrome oxide coating couple. It has been reported previously that chrome oxide (Cr_2O_3) appears to show poor sinterability [32] and may be adversely affecting the formation of tribo-films on tufts worn against chrome oxide coating.

The data suggest that the formation of a stable and continuous tribo-film is dependent on the availability and sinterability of the wear debris. Sintering is promoted by high temperature, small particle sizes and pressure. All of this clearly indicates that the sliding speed and hence the interfacial temperature along with the availability of debris are the key factors affecting the formation and nature of the tribo-films. Furthermore, the stability of these films increase with sliding speeds and may be the cause of the observed inverse relationship between SWR and sliding speed.

It is this formation, delamination and entrainment of tribo-films and debris which makes the observed wear mechanisms different from what has been reported in the literature. Despite the high speeds involved in these tests, the lack of expulsion of debris from the wear interface results in mechanisms such as those reported by Jiang et al. [23] and [24], normally associated with high temperature, low speed sliding, to be present here. Unlike the mild and severe oxidation models

reported by Lim and Ashby [30], the wear mechanisms observed on the bristle tufts appear to be more complex and show strong dependence on the nature of the tribo-films formed.

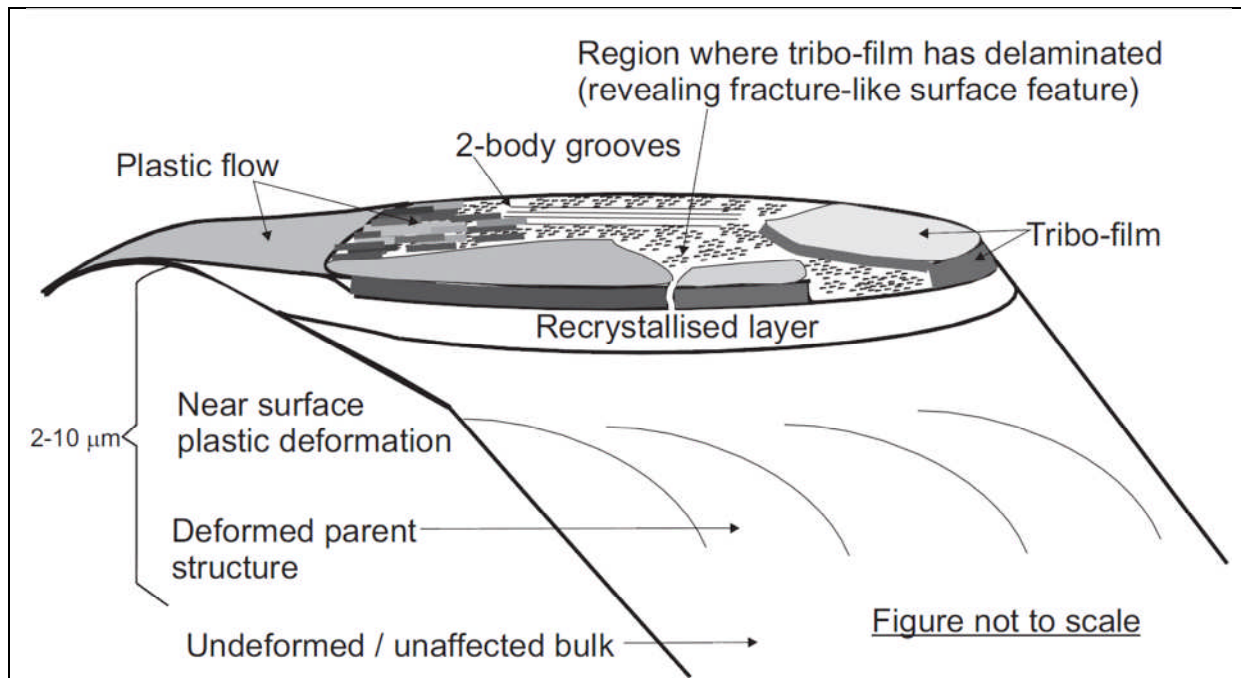


Figure 11: Schematic of a bristle showing a summary of the features observed on worn tufts

Conclusions

The wear characteristics of brush seals depend significantly on the ability of the surfaces to form tribo-films. In general, the wear mechanisms can be characterised in terms of the existence and stability of any tribo-films formed and notably low wear is promoted by the existence of a stable film.

The formation of a stable and continuous tribo-film was found to be dependent on the availability and sinterability of the wear debris. While the nitrided steel counterface provided Fe-rich debris allowing the formation of tribo-films on the bristle surfaces, the same was not the case with the chrome oxide coated counterface leading to greater wear rates being observed in bristles worn against the chrome oxide coating.

As sintering is promoted by high temperature, the stability of these tribo-films increase with sliding speeds and appears to cause the observed inverse relationship between specific wear rate (SWR) and sliding speed.

Thermal behaviour at the wear interface is dominated by frictionally generated heat. Evidence of plastic flow on the worn surfaces and sub-surface recrystallisation suggest the presence of temperatures probably close to 1000 °C at the interface. Microstructural examination also shows that these features are limited to a few microns from the wear interface which indicates the presence of a steep thermal gradient along the bristle tufts.

Acknowledgments

The authors would like to acknowledge Technology Strategy Board (UK) and Rolls-Royce plc for funding this work through the SILOET research programme and in particular Professor Terry Jones (University of Oxford), Chris Enderby and the late Jim Forfar (Rolls-Royce) for identifying the need and securing funding to start this project. The authors also like to thank Drs Hugh Bishop and Alison Crossley (Oxford Materials) for providing SIMS data and Dr Kalin Dragnevski and Professor Alan Cocks (Department of Engineering Science) for granting access to SEM and profilometry facilities. The authors would like to thank Mr Leo Verling for fabricating the rig and test samples.

References

- [1] Steinetz BM, Hendricks RC, Munson J. Advanced Seal Technology Role in Meeting Next Generation Turbine Engine Goals. Cleveland, Ohio: NASA, Lewis Research Centre; 1998. Report No.: NASA / TM-1998 -206961. Sponsored by NATO Research and Technology Agency, Toulouse, France.
- [2] Fellenstein JA, Dellacorte C. A new tribological test for candidate brush seal materials evaluation. *Tribol Trans* 1996;39:173–9.
- [3] Conner K.J, Childs DW. Rotordynamic and leakage characteristics of a 4-stage brush seal. Final Report, 30 Oct. 1988 - 30 Aug. 1992 Texas A&M Univ., College Station. Turbomachinery Labs. Final report. Ohio: Wright Laboratory, AFMC, Wright-Patterson Air Force Base; 1992. Report No.: WL-TR-92-2125.
- [4] Hawthorne HM. Brush-on-disc simulation tribotesting of materials for gas turbine-compliant seal components. *Tribol Int* 1994;27:87–95.
- [5] Bowden FP, Tabor D. The friction and lubrication of solids. Oxford, England: Clarendon Press; 1950.
- [6] Archard JF. The temperature of rubbing surfaces. *Wear* 1959;2:438–55.
- [7] Blok H. The flash temperature concept. *Wear* 1963;6:483–94.
- [8] Ashby MF, Abulawi J, Kong HS. Temperature maps for frictional heating in dry sliding. *Tribol Trans* 1991;34:577–87.
- [9] Archard JF, Hirst W. The wear of metals under unlubricated conditions. *Proc R Soc London A* 1956;236:397–410.
- [10] Hirst W, Lancaster JK. The influence of oxide and lubricant films on the friction and surface damage of metals. *Proc R Soc London A* 1954;223:324–38.
- [11] Hirst W, Lancaster JK. Surface film formation and metallic wear. *J Appl Phys* 1956;27:1057–65.

- [12] Hirst W, Lancaster JK. The influence of speed on metallic wear. *Proc R Soc London A* 1960;259:228–41.
- [13] Lancaster JK. The formation of surface films at the transition between mild and severe metallic wear. *Proc R Soc London A* 1963;273:466–83.
- [14] Lancaster JK. The influence of temperature on metallic wear. *Proc Phys Soc London B* 1957;70:112–8.
- [15] Cocks M. The role of atmospheric oxidation in high speed sliding phenomena. *J Appl Phys* 1957;28:835–43.
- [16] Cocks M. The role of atmospheric oxidation in high speed sliding phenomena -II. *Tribol Trans* 1958;1:101–7.
- [17] Rigney DA, Hirth JP. Plastic deformation and sliding friction of metals. *Wear* 1979;53:345–70.
- [18] Rigney DA, Chen LH, Naylor MGS, Rosenfield AR. Wear processes in sliding systems. *Wear* 1984;100:195–219.
- [19] Inman IA, Datta S, Du HL, Burnsell-Gray JS, Luo Q. Microscopy of glazed layers formed during high temperature sliding wear at 750 °C. *Wear* 2003;254:461–7.
- [20] Kato H, Komai K. Tribofilm formation and mild wear by tribo-sintering of nanometer-sized oxide particles on rubbing steel surfaces. *Wear* 2007;262:36–41.
- [21] Kato H, Sasase M, Suiya N. Friction induced ultra-fine and nanocrystalline structures on metal surfaces in dry sliding. *Tribol Int* 2010;43:925–8.
- [22] Stott FH, Wood GC. The influence of oxides on the friction and wear of alloys. *Tribol Int* 1978;11(4):211–8.
- [23] Jiang J, Stott FH, Stack MM. A mathematical model for sliding wear of metals at elevated temperatures. *Wear* 1995;181-3:20–31.
- [24] Jiang J, Stott FH, Stack MM. Some frictional features associated with sliding wear of nickel-based alloy N80A at temperatures to 250 °C. *Wear*. 1994;176:185–94.
- [25] Montgomery RS. Friction and wear at high sliding speeds. *Wear* 1976;36:275–98.
- [26] Philippon S, Sutter G, Molinary A. An experimental study of friction at high sliding speeds. *Wear* 2004;257:777–84.
- [27] Qiu M, Zhang YZ. Effect of different atmospheres on dry friction behaviour of steel sliding against brass at high speed. *Chin Sci Bull* 2009;4589–93.
- [28] Qiu M, Zhang YZ, Yang JH, Zhu J. Microstructure and tribological characteristics of Ti6Al4V alloy against GCr15 under high speed dry sliding. *Mat Sci Eng A* 2006;483:71–5.
- [29] Song Y, Yu H, Mao ZM. Wear behaviour of WCp/Fe-C composites under high speed dry sliding. *J Mater Sci* 2008;43:2686–92.

- [30] Lim SC, Ashby MF. Overview no. 55 wear-mechanism maps. *Acta Metall* 1987;35:1–24.
- [31] The American Society of Mechanical Engineers. Test Uncertainty. ASME PTC 19.1,: ASME; 2005.
- [32] Inman IA, Datta PK, Du HL, Burnell-Gray JS, Pierzgalski S, Luo Q. Studies of high temperature sliding wear of metallic dissimilar interfaces. *Tribol Int* 2005;38:812–23.